PIER M

(Received 8 December 2023, Accepted 22 February 2024, Scheduled 3 March 2024)

Research on Perspective Imaging Method of Building Structure Based on Multipath Information

Zhong-Yu Liu[1], Ya-Xing Qin[1], Li-Xin Guo[1,*], Ren-Jiang Zhu[1], Zhi-Gang Zhong[2], Zuo-Yong Nan[2], Ya Wang[2], and Ling-Feng Shen[2]

[1]*School of Physics, Xidian University, Xi'an 710071, China*
[2]*China Information Technology Designing & Consulting Institute CO. LTD., Beijing 100080, China*

ABSTRACT: The internal structural details of unknown structures are very helpful to our personnel in carrying out activities during anti-terrorism operations and emergency disaster relief operations in urban environments. According to multipath identification and propagation mechanism separation technology, a building structure perspective imaging algorithm based on the ray-tracing model is proposed in this paper by making full use of the rich multipath delay power spectrum information and gradually filtering the multipath. Based on the imaging results taking overall consideration of all the propagation factors involved, the presented study is used to obtain the intricate geometric structure of indoor buildings. The original approach is then verified by using measured data, and the proposed algorithm is further optimized by extracting the internal wall structure of the building scene based on the Hough transform algorithm. In comparison with the real wall of the building, the average error of the inverse building wall position using simulated data is 0.071 m, and the average error of the inverse building wall position using the measured data is 0.355 m.

1. INTRODUCTION

With the development of electronic information technology, electromagnetic perspective has been a relatively active and novel topic since it was proposed to determine the environmental structure information of buildings and green belts in the area by the propagation law of electromagnetic waves in different areas, which has a large demand not only in anti-terrorism and rescue, but also increasingly in the civil field and disaster relief [1]. In counter-terrorism operations and urban combat, if we can obtain the location of terrorists and the internal structure information of buildings in advance, it will help our combatants in their actions; in the case of sudden disasters, obtaining the location of victims and the damage of buildings can reasonably arrange rescuers for rescue, thus maximizing the safety of people's lives.

The most typical means of using the propagation characteristics of electromagnetic waves to obtain information about the internal structure of a building is the through-wall radar imaging method [2, 3], whose transceiver mode is generally the antenna located on the same outside of the building, using the reflected echo information collected by the motion transceiver antenna involved in the role of the internal scene of the building to complete the perspective imaging of the internal structure. At present, the main use of reflected wave signals through the wall imaging methods is mainly reverse projection algorithm, time inversion algorithm [4], compression perception algorithm, and inverse scattering transformation method.

The TAM-BP imaging algorithm is a research on radio wave ground exploration, and Jamshidi-Zarmehri et al. conducted a comprehensive exploration of radio wave penetration through walls [5]. Zhang et al. proposed a delay and amplitude corrected back projection (BP) algorithm in order to solve the probability problem of multiple targets going undetected by wall radar imaging (TWRI) in ultra-wideband (UWB) [6]. Considering the electromagnetic propagation characteristics of electromagnetic waves in planar multilayer media, scholars from the National University of Defense Technology proposed a time-delay amplitude modified BP algorithm for detecting targets in multilayer media, and Gao et al. proposed a hybrid time-reversal (TR)-reversal time-shift (RTM) method to localize targets in bilayer media [7]. Prada et al. proposed a time-reversal operator decomposition method [8]. Rasekh et al. introduced a new time inversion technique based on independent component analysis [9]. Levaris and Devancy proposed time-reversal multisignal classification method [10]. Lagunas et al. used sparse reconstruction techniques to reconstruct wall echoes by processing the echo time-domain signals and reconstructing walls using linear structures [11]. Jin et al. used the coherence factor weighting algorithm in traditional through-wall radar imaging to perform sparse reconstruction of building structures [12]. Zhao et al. used low-rank and sparse models to extracted wall echoes from radar signals [13] and used a sparse reconstruction method with full-variance regularization, which can effectively reduce the loss due to target discrepancy inside the building. Poli et al. linearized the equations using the Born approximation [14] and dealt with the backscatter imaging problem in methods such as compressed sensing.

The RF laminar imaging [15] method based on transmitted wave signals mainly uses the received signal strength information to reconstruct the internal scene structure of a build-

* Corresponding author: Li-Xin Guo (lxguo@xidian.edu.cn).

TABLE 1. Summary table of different imaging techniques.

	Through-the-Wall Radar	RF chromatography	This paper
Main imaging targets	Static single target behind the wall	Internal wall structure	Internal wall structure
Source of imaging data	Reflected wave time delay power spectrum	Transmitted wave power	Multipath time delay power spectrum
Measuring method	Ipsilateral multi-view scanning	Contralateral multi-view scanning	Fixed multi-transmitter multi-receiver
Limitations	Need to know wall thickness, dielectric constant	Lack of phase information of the signal, resulting in poor imaging	High time delay resolution requirements for multipath measurement equipment

ing. Due to the different attenuations of electromagnetic waves when they penetrate different media, the signal attenuation rate in space can be used to reconstruct the information of the internal wall layout of the building. The transmitting and receiving antennas are aligned along the outside of the building in parallel to transmit the received signal, and the internal geometry of the scene is obtained by inverting the spatial distribution of the signal attenuation rate [16].

Mostofi et al. at the University of New Mexico constructed a distribution map of the received signal strength to a fixed station by compressed sensing techniques [17], leveraging the sparse representation of channel spatial variations, and proposed a signal reconstruction interference cancellation method based on an incomplete measurement set to obtain the strength distribution of received signals inside a building scene. In 2017, Karanam and Mostofi et al. [18], for a constructed $2.96\,\mathrm{m} \times 2.96\,\mathrm{m} \times 0.4\,\mathrm{m}$ cubic building scene, used an unmanned aerial vehicle (UAV) orbit to collect WiFi signals and transformed them into a minimized 3D full variance problem using the Wentzel-Kramers-Brillouin (WKB) linear approximation method, and subsequently proposed a method based on Markov random field modeling, circular confidence propagation, and sparse signal processing for 3D wireless power measurement imaging. In 2020, Guo et al. [19] of Chinese Academy of Sciences proposed the use of reweighted full variance with prior information regularization algorithm. The results showed that the algorithm could obtain better results in terms of root-mean-square error and structural similarity, and could preserve the wall structure orientation more accurately. Subsequently, Guo et al. [20] processed the received signal by pulse compression, which allowed the multipath signal to be separated from the direct transmitting wave, and reconstructed the scene layout structure using an improved total variation regularization algorithm for an experimental scene with only horizontal and vertical walls.

Building-based perspective research has had rapid development in recent years, and common methods include reflected-wave signal-based through-wall radar imaging method and transmitted-wave signal-based RF laminar imaging method. The first method requires the transceiver antenna to be located on the same side of the building, while the second method only uses the amplitude information of the transmitted wave signal and lacks signal phase information. Table 1 compares the differences between the above imaging methods and the methods described in this paper.

In view of the limitations of the above algorithm, the algorithm in this paper makes the following optimizations and innovations:

1) Compared with the traditional imaging method using a single path such as reflection path or transmission path, this paper is based on rich multipath time delay power spectrum information, making full use of the electromagnetic propagation characteristics of the whole building scene, and can successfully invert the internal wall structure of complex multi-room buildings.

2) Compared with traditional imaging methods that use parallel same side or opposite side scanning sampling, this paper achieves layout imaging of complex building scenes when the transmitting and receiving antenna positions move arbitrarily.

The algorithm in this paper utilizes rich multipath time delay power spectrum information, adopts multipath identification and propagation stripping techniques to obtain the multipath information of transmission path, reflection path, and diffraction path, filters the multi-paths one by one according to the ray tracing model, fuses the imaging results under different paths, and obtains the indoor complex building geometry structure. Finally, the original algorithm will be verified by using the measured data; the internal wall structure of the building scene will be extracted based on the measured data using the Hough transform algorithm; and the original algorithm will be further optimized.

2. ALGORITHM MODEL

The transmitting and receiving antennas are arranged around the building, and the ray-tracing model is used to predict the propagation process. The three main propagation mechanisms that may be involved in the propagation process are reflection, diffraction, and transmission, as shown in Figure 1. Suppose that the coordinates of the transmitting point are $T_x(x_t, y_t, z_t)$; emission frequency is f; the coordinates of the receiving point are $R_x(x_r, y_r, z_r)$; P_{ref}, P_{dif}, P_{tr} denote the reflection, diffraction, and transmission points acting on the building scene, respectively.

The multipath time delay power spectrum collected by the receiver point is processed and given in the form of (time delay - power), assuming that the multipath information collected by the receiver point is $\begin{pmatrix} \tau_1 & \tau & \cdots & \tau_{N-1} & \tau_N \\ p_1 & p_2 & \cdots & p_{N-1} & p_N \end{pmatrix}$. Taking

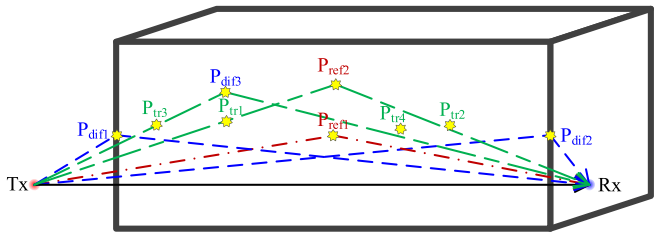

FIGURE 1. Building scene multipath schematic.

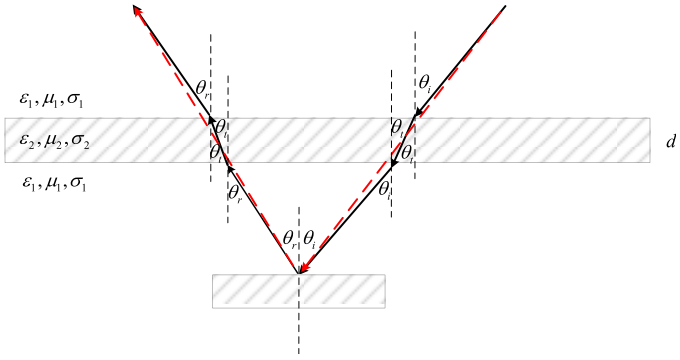

FIGURE 2. Transmission path wall time delay compensation schematic.

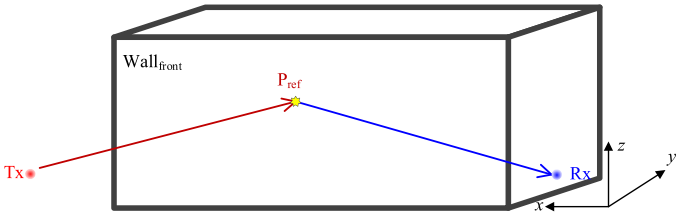

FIGURE 3. Reflection point extraction schematic.

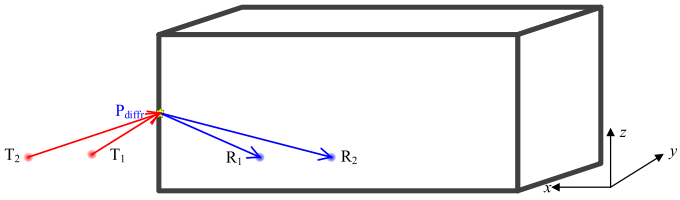

FIGURE 4. Schematic diagram of diffraction point extraction.

Figure 1 as an example, the paths involved in the propagation process include direct paths, wall primary reflection paths, wall corner primary diffraction paths, reflection paths through the front wall on the back wall, diffraction paths through the front wall on the back wall, etc., and their corresponding multipath information is $\begin{pmatrix} \tau_{dir} & \tau_{ref1} & \tau_{dif1} & \tau_{dif2} & \tau_{ref2} & \tau_{dif3} \\ p_{dir} & p_{ref1} & p_{dif1} & p_{dif2} & p_{ref2} & p_{dif3} \end{pmatrix}$.

2.1. Multipath Ray Path Processing

2.1.1. Transmission Path Wall Time Delay Compensation

As shown in Figure 2, the path of the electromagnetic wave penetrating the front wall of thickness d is shown, and the reflection occurs on the back wall with a reflection time delay of τ. The angular deflection of the electromagnetic wave at the incident interface makes it very inconvenient to calculate the coordinates of the reflection point; to make the calculation more convenient for the time delay of the electromagnetic wave through the wall plus a time delay compensation, assume that the path of the electromagnetic wave through the wall is not angular deflection [20]. At this point, the propagation path is shown in the dashed line in Figure 2.

2.1.2. Extraction of Reflective Points

As shown in Figure 3, the receiving antenna is located on the same side of the building as the transmitting antenna, where the coordinates of the transmitting point are $T_x(x_t, y_t, z_t)$, and the coordinates of the receiving point are $R_x(x_r, y_r, z_r)$.

In the actual measurement process, the transmitting and receiving antennas are located at the same height; directional antennas are used; and wave-absorbing materials are arranged at suitable locations around the transmitting and receiving antennas, which can shield the direct line-of-sight path, the primary ground reflection path of the transmitting point-ground-receiving point and other interference such as ray paths involved in the buildings in the non-to-be-measured area.

Assuming that the building wall is perpendicular to the ground and the coordinates of the wall reflection point $P_{ref}(x_{ref}, y_{ref}, z_{ref})$, outer normal vector of the front wall surface $\hat{n}_{front}(x_{front}, y_{front}, z_{front})$. Therefore, the incident direction vector is $\overrightarrow{T_x P_{ref}}$; the reflection direction vector is $\overrightarrow{P_{ref} R_x}$; the direct path direction is $\overrightarrow{T_x R_x}$; the time delay for the arrival of the reflection path is τ_{ref}.

When the transmitting and receiving antennas are located at the same height, that is, when $z_t = z_r$, if the reflection condition is met, the coordinates of the reflection point can be obtained by solving Equation (1). The derivation process of formulas for calculating the coordinates of reflection and diffraction points is detailed in [21].

$$\begin{cases} x_{ref} = \frac{1}{4}\dfrac{x_t - \frac{x_t+x_r}{y_t+y_r}y_t \pm \sqrt{\left(\frac{x_t+x_r}{y_t+y_r}y_t - x_t\right)^2 - \left(1+\left(\frac{x_t+x_r}{y_t+y_r}\right)^2\right)\left(x_t^2+y_t^2-\tau_{ref}^2 \cdot v_c^2\right)}}{1+\left(\frac{x_t+x_r}{y_t+y_r}\right)^2} \\ y_{ref} = -\frac{1}{4}\frac{x_t+x_r}{y_t+y_r}\dfrac{x_t - \frac{x_t+x_r}{y_t+y_r}y_t \pm \sqrt{\left(\frac{x_t+x_r}{y_t+y_r}y_t - x_t\right)^2 - \left(1+\left(\frac{x_t+x_r}{y_t+y_r}\right)^2\right)\left(x_t^2+y_t^2-\tau_{ref}^2 \cdot v_c^2\right)}}{1+\left(\frac{x_t+x_r}{y_t+y_r}\right)^2} \end{cases} \quad (1)$$

2.1.3. Extraction of Diffraction Points

As shown in Figure 4, the receiving antenna is located on the same side of the building as the transmitting antenna, where the coordinates of the transmitting point are $T_1(x_{t1}, y_{t1}, z_{t1})$, $T_2(x_{t2}, y_{t2}, z_{t2})$. The coordinates of the receiving points are $R_1(x_{r1}, y_{r1}, z_{r1})$, $R_2(x_{r2}, y_{r2}, z_{r2})$.

When the transmitting antenna is located at T_1 and the receiving antenna located at R_1, assuming that the building wall is perpendicular to the ground, the time delay of arrival at the receiving point R_1 is τ_{dif1}. The wall prism is around the projection point $P_{dif}(x_{dif}, y_{dif}, z_{dif})$. Therefore, the incident direction vector is $\overrightarrow{T_1P_{dif}}$, the outgoing direction vector at the receiving point R_1 is $\overrightarrow{P_{dif}R_1}$; and the direct path direction vector is $\overrightarrow{T_1R_1}$.

Assume that the height of the transceiver antenna is the same as the height of the diffraction point, i.e., $z_t = z_{r1} = z_{r2} = z_{dif}$. The sum of the distance between the target point and transmitting and receiving antennas can be calculated according to the round-trip time delay of the echo between the transmitting point, receiving point, and diffraction point. Therefore, in the case where the position of the transmitting and receiving antennas and the sum of the distances from the target point to the transmitting and receiving antennas are known, an ellipse can be constructed and only constructed from the transmitting and receiving antenna coordinates and the signal propagation distance, and the two focal coordinates of the ellipse are the transmitting and receiving antenna coordinate positions during the movement.

The first elliptic expression can be obtained when the transceiver point is located at T_1R_1, and the second elliptic expression can be obtained when the transceiver point is located at T_2R_2. By combining two equations, the coordinates of the diffraction point can be obtained by solving Equation (2).

$$\begin{cases} x_{dif} = \pm\frac{\tau_{dif1}\cdot\tau_{dif2}\cdot v_c}{2} \\ \qquad \sqrt{\frac{-\left(\left(\tau_{dif1}^2\cdot v_c^2-\left|\overrightarrow{T_1R_1}\right|^2\right)-\left(\tau_{dif2}^2\cdot v_c^2-\left|\overrightarrow{T_2R_2}\right|^2\right)\right)}{\left(\tau_{dif1}^2\cdot\left(\tau_{dif2}^2\cdot v_c^2-\left|\overrightarrow{T_2R_2}\right|^2\right)-\tau_{dif2}^2\cdot\left(\tau_{dif1}^2\cdot v_c^2-\left|\overrightarrow{T_1R_1}\right|^2\right)\right)}} \\ y_{dif} = \pm\frac{1}{2}\sqrt{\frac{\left(\tau_{dif1}^2\cdot v_c^2-\left|\overrightarrow{T_1R_1}\right|^2\right)\cdot\left(\tau_{dif2}^2\cdot v_c^2-\left|\overrightarrow{T_2R_2}\right|^2\right)\cdot\left(\tau_{dif1}^2-\tau_{dif2}^2\right)}{\tau_{dif1}^2\cdot\left(\tau_{dif2}^2\cdot v_c^2-\left|\overrightarrow{T_2R_2}\right|^2\right)-\tau_{dif2}^2\cdot\left(\tau_{dif1}^2\cdot v_c^2-\left|\overrightarrow{T_1R_1}\right|^2\right)}} \end{cases} \tag{2}$$

2.2. Multipath Ray Path Identification

According to the different propagation mechanisms involved in the propagation process at the receiving point, the possible ray paths received around the building can be divided into seven categories: direct line-of-sight path, direct non-line-of-sight path, one reflection path, one diffraction path, two transmissions and one reflection path, two transmissions and one diffraction path, and other combined paths. By matching the multipath time delay power information at the receiving point with the transmission loss, reflection loss, diffraction loss, etc., the source of the propagation mechanism of multipath at the receiving place can be judged, so as to realize the extraction of the interaction point under different propagation mechanisms.

In multipath ray identification, the first is the matching of multipath delay and path distance, and the second is the matching of multipath power and the calculated multipath power. If both can be matched, it means that this path is identified. The following is the calculation method for matching direct line-of-sight path and once-reflected path, and the same calculation method for matching direct non-line-of-sight path, once-around path, twice transmitted and once-reflected path, and twice transmitted and once-around path.

For example, in a direct line of sight path, if the multipath information at the receiver satisfies Equation (3), it can be considered as a direct line of sight path.

$$\begin{cases} \sqrt{(x_t - x_r)^2 + (y_t - y_r)^2 + (z_t - z_r)^2} = \tau \cdot v_c \\ p_r = p_t - L_d \end{cases} \tag{3}$$

where p_t, p_r denote the powers at transmission and reception points; τ denotes the time delay at receive; and L_d denotes the loss in the direct path.

Again, the multipath information at the reception in a primary reflection path can be considered as a primary reflection path if the following equation is satisfied.

$$\begin{cases} p_r = p_t - L_a - L_s - L_r \\ \tau \cdot v_c = \sqrt{(x_t - x_{ref})^2 + (y_t - y_{ref})^2 + (z_t - z_{ref})^2} \\ \qquad\qquad + \sqrt{(x_r - x_{ref})^2 + (y_r - y_{ref})^2 + (z_t - z_{ref})^2} \end{cases} \tag{4}$$

According to the above, six paths can initially reconstruct part of the geometric structure of the building scene, based on the reconstructed scene structure, and the other combined paths are split into combinations of the above paths. The corresponding paths can be identified by matching the corresponding time delay power.

With the transceiver antenna position fixed, the reflection point is on the vertical bisector of its transceiver antenna, and the diffraction point is on the ellipse with the transceiver antenna as the focus. Moving the position of the transceiver antenna, the coordinates of the reflection point and diffraction point can be solved to calculate the interaction point, which is the wall and corner geometry of the building scene. Probabilistic accumulation of the set space of reflection and diffraction points is performed to finally obtain the set with the presence of building media in this horizontal section.

2.3. Optimal Extraction of Building Geometry

Using the collected multipath time delay spectrum data, the prototype of the building wall structure can already be obtained by the above imaging algorithm. In order to better get the building wall location, Hough Transform (HF) can be used to extract the wall structure in it.

The Hough transform can detect straight lines from binary images, as shown in Figure 5. After the Hough transform, each point (x, y) in the image space is mapped to a curve in (r, θ) space, and a straight line in the (x, y) space coordinate system is obtained by the number of crossings of all lines in (r, θ)

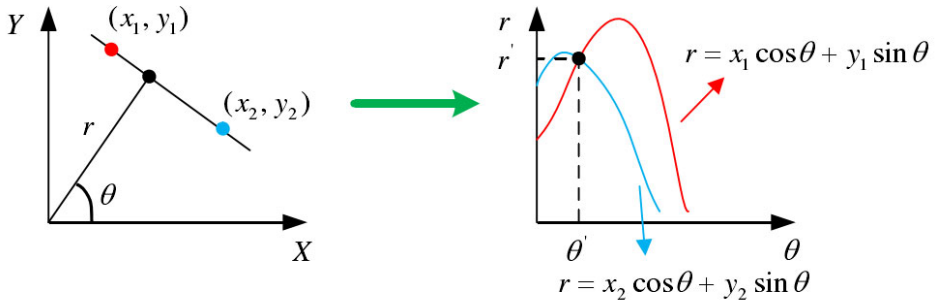

FIGURE 5. Linear detection using Hough transform.

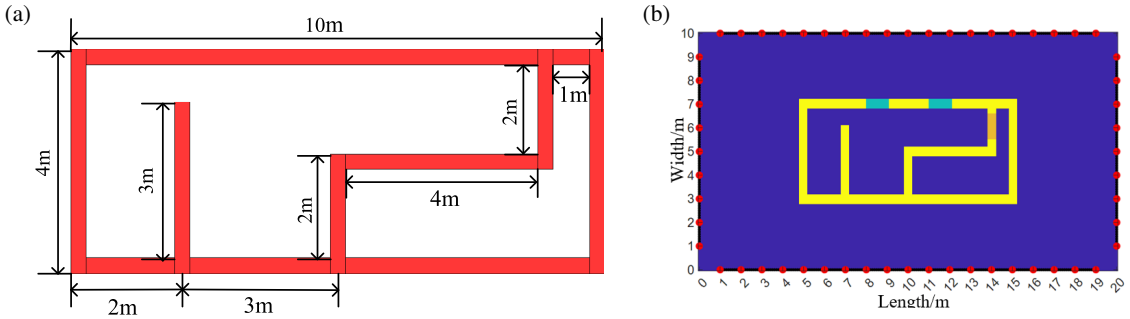

FIGURE 6. Building scene plan: (a) structure plan and (b) location map of transmitting and receiving antennas with a segmentation accuracy of 0.1 m.

space. In the actual wall penetration scenario, the target wall is approximated as a series of line segments on the image, which can then be detected on the image using the Hough transform.

3. SIMULATION RESULTS

The structure of the building scene to be inverted is shown in Figure 6(a). The specification of the scene to be measured is 20 m × 10 m; the thickness of all walls is 0.3 m; the relative permittivity is 6; the conductivity is 0.136 S/m; and the transmitting frequency is 4 GHz, and its scene modeling at the profiling accuracy of 0.1 m is shown in Figure 6(b). The transmitting and receiving antennas are arranged around the building. There are 56 transmitting points, and the receiving antennas move at 0.1 m on the same side of the transmitting antennas. The red dots around the building indicate the transmitting antennas, and the black dots indicate the receiving antennas. In theory, the denser the arrangement of the transmitting and receiving antennas is, the better the imaging results are. However, considering the huge amount of data and computational speed, it is more appropriate to set the spacing between the transmitting antennas to 1 m and the receiving antennas to 0.1 or 0.2 m.

Through the multipath information received at the transceiver antenna position shown in Figure 6(b), the primary reflection path, two transmission and primary reflection paths, primary diffraction path, and two transmission and primary diffraction paths are extracted. The primary reflection points involved in the propagation of the building scene are calculated based on all the primary reflection paths, and the primary reflection points involved in the propagation of the building scene are calculated based on all the two transmission and primary reflection paths. The primary reflection point is calculated based on all primary diffraction paths; the primary diffraction point is calculated based on all primary diffraction paths; and the primary diffraction point is calculated based on all twice-transmission and primary diffraction paths for propagation inside the building scene.

The imaging results of the primary reflection path, two transmission and primary reflection paths, primary diffraction path, and two transmission and primary diffraction paths are superimposed in the above, and the imaging results of the integrated path are obtained, as shown in Figure 7(a). Assuming that the thickness of the building wall is 0.3 m, the imaging schematic of the primary diffraction path under the consideration of the wall thickness is obtained, as shown in Figure 7(b); the mean square error between its reconstructed image and the original image is 0.0244; and the structural similarity is 0.9981.

4. MEASUREMENT VERIFICATION

4.1. Test Environment

A multi-room building scene was selected near Bai Village in Liquan County, Xi'an, and its geometry is shown in Figure 8(a). The length dimension specification of its geometric structure is shown in Figure 8(b).

4.2. Experimental Equipment

The measurement equipment is mainly used to measure the multipath of the channel by receiving the signal sent from the

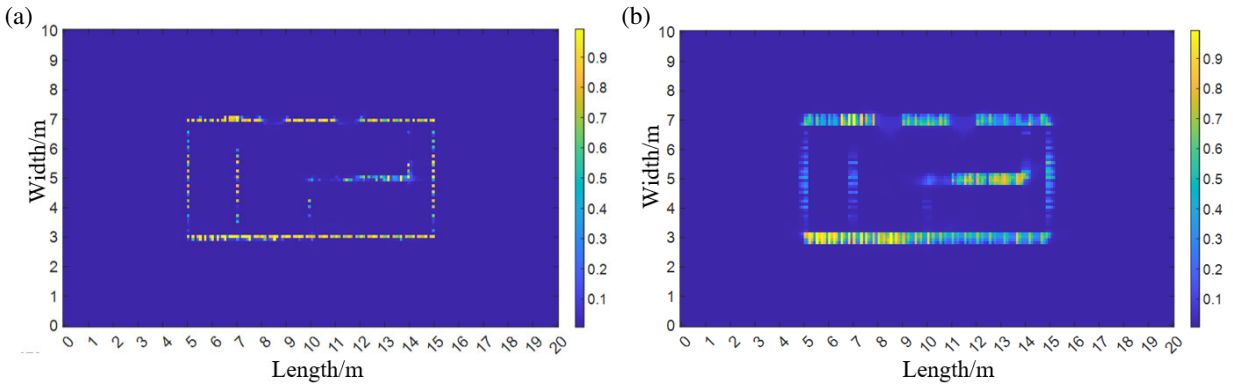

FIGURE 7. Multipath comprehensive imaging result map: (a) regardless of wall thickness and (b) considering wall thickness.

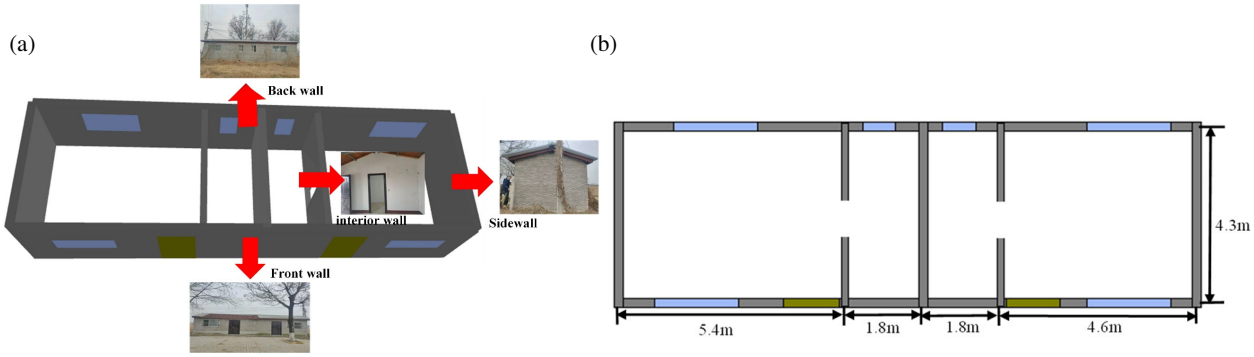

FIGURE 8. Multi-room building structure: (a) 3D schematic diagram and (b) plan sketch.

TABLE 2. List of measurement system equipment.

Serial number	Name	Quantity	Instruction
1	Transceiver	2 units	
2	Power Amplifier	1 units	
4	Directional Antenna	2 units	Mainly used as transmitting antenna
5	Omni-directional Antenna	2 units	Mainly used as receiving antenna
6	GPS antenna	2 units	For transceivers
7	Mobile Power	2 units	For transceivers
8	Removable bracket	2 units	For transceivers

fixed transmitter and resolving the multipath delay and power in it. The main system components of the equipment are shown in Table 2.

Figure 9(a) shows the physical diagram of the transceiver, and the multipath measurement system shown in Figure 9(c) is built according to the schematic diagram shown in Figure 9(b), in which the transmitting signal frequency of the signal transceiver is 4000–4200 MHz; the sampling rate is 250 MHz; the time delay resolution is 4 ns; the time delay resolution after processing by super-resolution algorithm is 1 ns. The transmitting antenna uses a horn antenna, and its gains at 4000 MHz, 4100 MHz, and 4200 MHz are 20.54 dBi, 20.83 dBi, and 20.97 dBi, respectively; the receiving antenna adopts omnidirectional antenna; and its gain in 4000–4200 MHz is 6 dBi. For multipath measurement experiments, it is best to use omnidirectional antennas for both transmission and reception, as data processing will be easier. However, due to laboratory equipment reasons, directional antennas are used for transmission here.

4.3. Measured Results

The raw multipath data collected and the multipath processed data processed by the super-resolution algorithm are shown in Figure 10, respectively.

It can be found that there are four received multipath signals, in order of the reflection path of the front wall, and the reflection path of the three inner walls. As the time delay difference between the corner diffraction path and the front wall reflection path is not large, the influence of the multipath device time delay resolution will show no diffraction path.

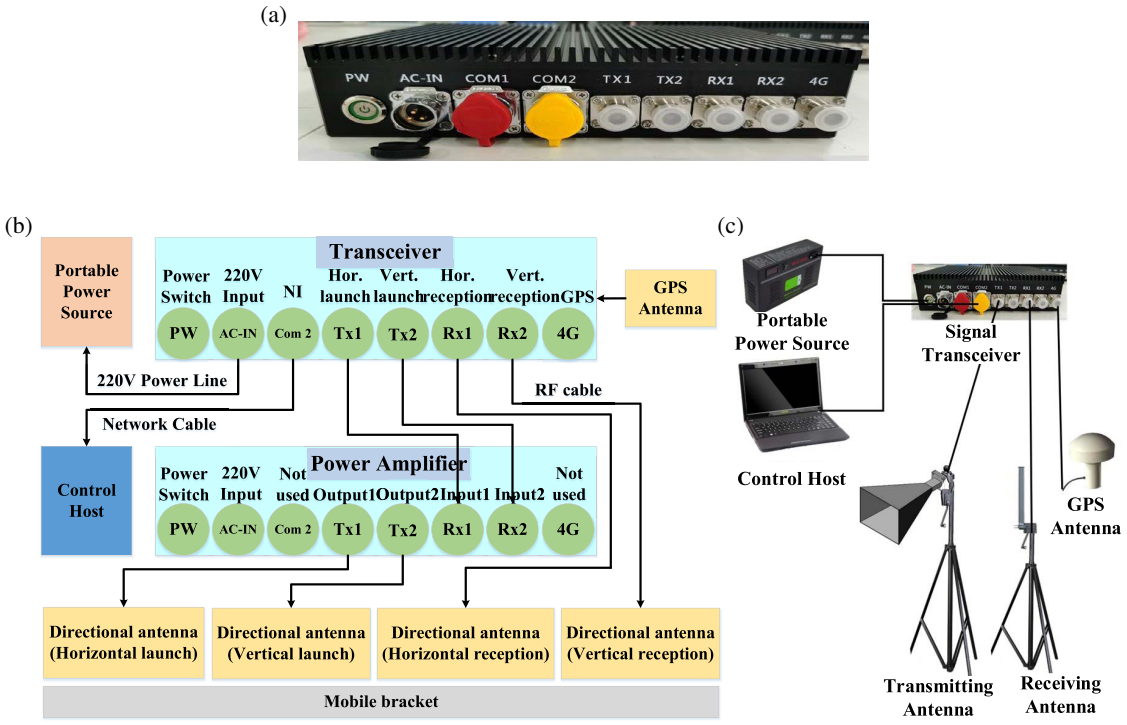

FIGURE 9. Schematic diagram of experimental system: (a) ransceiver physical object, (b) transceiver connection and (c) multipath testing system.

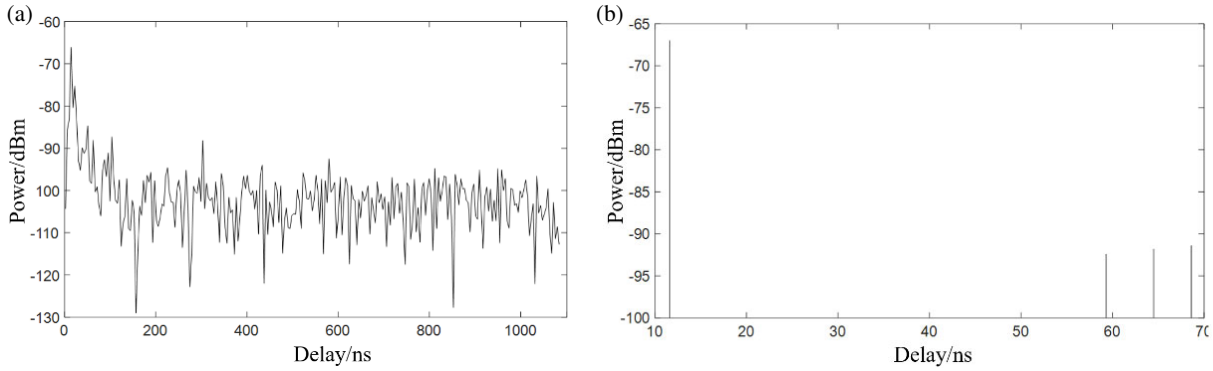

FIGURE 10. Transmitting and receiving multipath data with an interval of 1 m: (a) raw data and (b) processed data.

In the same side transceiver mode, the transmitter uses a horn antenna; the receiver uses an omnidirectional antenna; and the transceiver point on the same side of the wall is a set of sampling data. In the opposite side transceiver mode, both the transmitter and receiver use an omnidirectional antenna, and the transceiver point on the opposite side of the wall is a set of sampling data.

Four corner points are selected around the building as shown in Figure 11, are used as the reference points, and are fixed on the same horizontal plane by the Nealon line. As shown in the blue line in Figure 11, take the horizontal plane formed by the blue line as the reference plane, and restrict the transceiver antenna to move only on the blue line in the test.

In the actual measurement, in order to facilitate effective positioning of the antenna, the coordinates of the fall point of the plumb line are used as the water plane coordinates of the antenna, and the time delay and power calibration of the measurement equipment and the cable are carried out with this coordinate position before the experiment is started.

Measurements were performed on the front wall, side wall, and back wall separately, i.e., the transmitting antenna position was fixed, and the receiving antenna was moved at 0.1 m intervals on the same side. The transmitting and receiving antenna positions during the movement of the front wall are shown in Figure 12.

Simulation is performed at the location of the actual measurement point. According to the multipath time-delay power spectra acquired at different locations, the imaging results of reflection and diffraction paths at different positions are obtained by processing them using the algorithm of reflection and diffraction paths. The final simulation results of fusion imaging under multipath and multiple viewpoints are obtained by fusing dif-

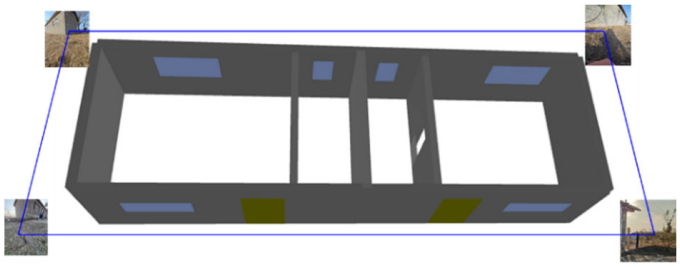

FIGURE 11. Schematic diagram of test reference surface.

FIGURE 12. Schematic diagram of the position of the transmitting and receiving antennas during the testing process.

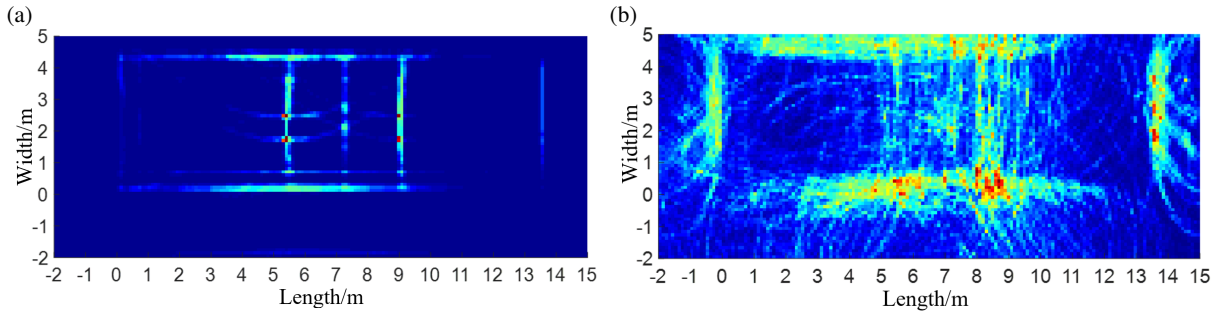

FIGURE 13. Multipath and multi view fusion imaging results: (a) simulation result and (b) measured results.

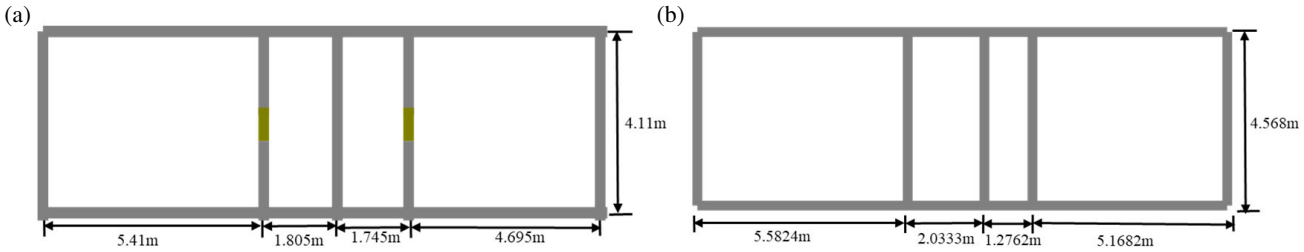

FIGURE 14. Extraction of wall structure by Hough transform: (a) simulation data and (b) measured data.

ferent reflection path imaging and wrap-around radiation path imaging together, as shown in Figure 13(a).

Similarly, based on the actual measured multipath delay power spectrum, the reflection path imaging results at different positions are obtained by processing according to the reflection path algorithm. The diffraction path imaging results at different positions are obtained by processing according to the diffraction path algorithm. The reflection path imaging results are integrated with the diffraction path imaging to obtain the fusion imaging results under multipath and multiview conditions.

Due to the limitation of penetration loss, the signal from the third wall inside the building is basically not received when the transceiver is placed outside the side wall. Therefore, the transmitter and receiver are placed at the front wall and the back wall, respectively, so that the third wall inside can participate in the electromagnetic wave propagation process to fuse the imaging results of the same side and opposite side transceivers, and get the final imaging results under multi-view multi-path, as shown in Figure 13(b).

4.4. Optimized Extraction

The wall structures inside the building are extracted by Hough transform for the simulated and measured images, as shown in Figure 14(a) and Figure 14(b), respectively.

Comparing the wall dimensions in the simulated and measured images with the real walls, the average error of the building wall dimensions obtained from the inversion of the simulation data is calculated to be 0.071 m, and the average error of the building wall dimensions obtained from the inversion of the measured data is 0.355 m.

5. CONCLUSION

In this study, the transmission path, reflection path, and diffraction path multipath information of the building scene is obtained using the multipath identification and propagation stripping techniques based on the outdoor-indoor-outdoor electromagnetic propagation prediction model of the ray-tracing algorithm. The interaction points of the corresponding paths in-

volved in the propagation in the building scene are then extracted, and the imaging study of the building layout is completed. The final imaging results of the building plan are produced by superimposing the imaging results of several paths, including one reflection path, two transmissions and one reflection path, one diffraction path, two transmissions, and one diffraction path. In order to achieve higher accuracy, future research will optimize the accuracy of the building interior structural perspective method by combining the directional measurement equipment and higher resolution multipath measurement equipment, and compare and analyze the imaging results with the results of the traditional imaging method.

ACKNOWLEDGEMENT

This work was supported in part by the key project of Social Governance and Scientific and Technological Support for Smart Society (Grant No. 2022YFC3301403), Key Basic Research Project of the Foundation Strengthening Program, and the Research Fund of Ministry of Education of China-China Mobile (Contract No. MCM20200302).

REFERENCES

[1] Saad, M., A. Maali, M. S. Azzaz, A. Bouaraba, and M. Benssalah, "Development of an IR-UWB radar system for high-resolution through-wall imaging," *Progress In Electromagnetics Research C*, Vol. 124, 81–96, 2022.

[2] Nkwari, P. K. M., S. Sinha, and H. C. Ferreira, "Through-the-wall radar imaging: A review," *IETE Technical Review*, Vol. 35, No. 6, 631–639, Nov. 2018.

[3] Jia, Y., L. Kong, and X. Yang, "A novel approach to target localization through unknown walls for through-the-wall radar imaging," *Progress In Electromagnetics Research*, Vol. 119, 107–132, 2011.

[4] Wu, P. and Z. Guo, "High-precision inversion of buried depth in-urban underground iron pipelines based on AM-PSO algorithm-for magnetic anomaly," *Progress In Electromagnetics Research C*, Vol. 100, 17–30, 2020.

[5] Jamshidi-Zarmehri, H., A. Akbari, M. Labadlia, K. E. Kedze, J. Shaker, G. Xiao, and R. E. Amaya, "A review on through-wall communications: Wall characterization, applications, technologies, and prospects," *IEEE Access*, Vol. 11, 127 837–127 854, 2023.

[6] Zhang, H., D. Li, J. Zhao, and H. Wang, "Time-delay and amplitude modified BP imaging algorithm of multiple targets for UWB through-the-wall radar imaging," *Journal of Information Processing Systems*, Vol. 13, No. 4, 677–688, 2017.

[7] Gao, X., H.-J. Yang, J. Ma, J.-H. Li, W. Wang, and C.-H. Wang, "The principle of detection and location of target in multi-layered media by TR-RTM mixed method," in *2019 13th Symposium on Piezoelectrcity, Acoustic Waves and Device Applications (SPAWDA)*, 1–4, Harbin, China, Jan. 2019.

[8] Prada, C., J.-L. Thomas, and M. Fink, "The iterative time reversal process: Analysis of the convergence," *The Journal of the Acoustical Society of America*, Vol. 97, No. 1, 62–71, 1995.

[9] Rasekh, P., M. Razavian, A. Torki, H. K. Rad, and R. Safian, "Single-antenna time-reversal imaging based on independent component analysis," *Progress In Electromagnetics Research M*, Vol. 44, 47–58, 2015.

[10] Levari, H. and A. J. Devancy, "The time-reversal technique re-interpreted: Subspace-based signal processing for multi-static target location," in *Proceedings of the 2000 IEEE Sensor Array and Multichannel Signal Processing Workshop*, 509–513, Cambridge, USA, 2000.

[11] Lagunas, E., M. G. Amin, F. Ahmad, and M. Nájar, "Sparsity-based radar imaging of building structures," in *2012 Proceedings of the 20th European Signal Processing Conference (EUSIPCO)*, 864–868, Bucharest, Romania, Aug. 2012.

[12] Jin, T. and Y. Song, "Sparse imaging of building layouts in ultra-wideband radar," *Journal of Radars*, Vol. 7, No. 3, 275–284, 2018.

[13] Zhao, J., L. Jin, and Q. Liu, "Through-the-wall radar sparse imaging for building walls," *The Journal of Engineering*, Vol. 2019, No. 21, 7403–7405, Nov. 2019.

[14] Poli, L., G. Oliveri, and A. Massa, "Microwave imaging within the first-order Born approximation by means of the contrast-field Bayesian compressive sensing," *IEEE Transactions on Antennas and Propagation*, Vol. 60, No. 6, 2865–2879, Jun. 2012.

[15] Cao, X., H. Yao, Y. Ge, and W. Ke, "A lightweight robust indoor radio tomographic imaging method in wireless sensor networks," *Progress In Electromagnetics Research M*, Vol. 60, 19–31, 2017.

[16] Jin, T., Y. Song, G. Cui, and S. Guo, "Advances on penetrating imaging of building layout technique using low frequency radio waves," *Journal of Radars*, Vol. 10, No. 3, 342–359, 2021.

[17] Mostofi, Y. and P. Sen, "Compressed mapping of communication signal strength," in *2008 IEEE Military Communications Conference*, 1–7, San Diego, USA, 2008.

[18] Karanam, C. R. and Y. Mostofi, "3D through-wall imaging with unmanned aerial vehicles using WiFi," in *Proceedings of the 16th ACM/IEEE International Conference on Information Processing in Sensor Networks*, 131–142, Pittsburgh, USA, 2017.

[19] Guo, Q., Y. Li, X. Liang, J. Dong, and R. Cheng, "Through-the-wall image reconstruction via reweighted total variation and prior information in radio tomographic imaging," *IEEE Access*, Vol. 8, 40 057–40 066, 2020.

[20] Guo, Q., Y. Li, X. Liang, J. Dong, and R. Cheng, "A novel CT-mode through-the-wall imaging method based on time delay estimation," *IEEE Geoscience and Remote Sensing Letters*, Vol. 18, No. 8, 1381–1385, 2020.

[21] Zhu, R., "Research on perspective imaging method of building structure," Ph.D. dissertation, Xidian University, Xi'an, 2022.